

RESTORATION AND ENHANCEMENT OF FINGERPRINT IMAGES USING *M*-LATTICE – A NOVEL NON-LINEAR DYNAMICAL SYSTEM

Alex Sherstinsky and Rosalind W. Picard

Media Laboratory, E15-383
Massachusetts Institute of Technology, Cambridge, MA 02139
shers@media.mit.edu and picard@media.mit.edu

ABSTRACT

We develop a method for the simultaneous restoration and halftoning of fingerprints using the “*M*-lattice”, a new non-linear dynamical system. This system is rooted in the reaction-diffusion model, first proposed by Turing to explain morphogenesis (the formation of patterns in nature). But in contrast with the general reaction-diffusion, the state variables of the *M*-lattice are guaranteed to be bounded. The *M*-lattice system is closely related to the analog Hopfield network and the cellular neural network, but has more flexibility in how its variables interact. These properties make it better suited than reaction-diffusion for several new engineering applications. The proposed method for enhancing fingerprints explores the ability of the *M*-lattice to form oriented spatial patterns (like reaction-diffusion), while producing binary outputs (like feedback neural networks). The fingerprints synthesized by the *M*-lattice retain and emphasize more of the relevant detail than do those obtained by adaptive thresholding, a common halftoning method employed in traditional fingerprint classification systems.

1. INTRODUCTION

The reaction-diffusion model was first proposed by Turing in 1952 in order to explain the growth of hydra tentacles. Subsequently, it has been used as a model for mammalian coating patterns, such as, for example, zebra stripes, leopard spots, *etc.* Until recently, reaction-diffusion systems have been researched predominantly by mathematical biologists working on theories of natural pattern formation and by chemists working on modeling the dynamics of complex chemical reactions [1], [2]. However, the past several years have seen a significant surge in interest in reaction-diffusion systems, primarily for exploiting them in the areas of computer graphics [3], [4] and image processing [5].

For pattern formation to occur, a reaction-diffusion system must exhibit local instability to small non-homogeneous perturbations. But practical considerations dictate that the system’s state variables should be bounded in the large-signal regime. A major difficulty associated with the reaction-diffusion paradigm is that it possesses the pattern-forming property only for a restricted class of non-linear reaction functions [6]. This drawback narrows the scope of the model’s engineering applications.

A common approach aimed at preventing numerical overflow caused by the instability of reaction-diffusion systems

has been to clip the magnitudes of the state variables by adding an “if” statement to the numerical method (*e.g.*, Forward Euler) used for solving the system of differential equations on the computer [4]. For some reaction-diffusion systems, this technique eventually manages to stop the state variables from changing between successive time steps. However, controlling a system of differential equations from within the numerical method destroys the mathematical integrity of the original dynamical system, making it hard to analyze and adapt to new applications.

The main contribution of this paper is the formulation of the “clipped *M*-lattice system” as a more practical and flexible extension of the reaction-diffusion model [7]. By using a warping function to facilitate boundedness, this new system allows more flexible non-linear interactions than the reaction-diffusion system. Furthermore, in contrast with the original reaction-diffusion system, convergence of the clipped *M*-lattice system to a fixed point has been observed in computer simulation for a large variety of non-linear observation functions. In order to account for some of these observations, we have proven the total stability of a subclass of the clipped *M*-lattice system [8]. The *M*-lattice system is closely related to the analog Hopfield network [9] and the cellular neural network [10], but has more flexibility in how its variables interact. The model’s ability to inherit the pattern-formation aspects of reaction-diffusion is illustrated in an application to the restoration and enhancement of scanned fingerprint images.

The rest of this document is organized as follows. Section 2 discusses the basic properties of the reaction-diffusion model. Section 3 reviews the *M*-lattice system. Section 4 derives the pattern-formation properties of one type of the clipped *M*-lattice system and applies it to the pre-processing of fingerprints. Section 5 summarizes the report.

2. REACTION-DIFFUSION

Turing’s last paper before his death was a first attempt to provide a scientific explanation for the dappled patterns of pigmentation in animals [1]. Many mammals have prominent coat markings. For example, zebras have stripes, giraffes have contoured patches, leopards and cheetahs have spots; the furs of many dogs and cats also display various forms of stripes and patches of different color. In addition, many tropical fish exhibit colorful patterns of spots and stripes.

Turing proposed to model nature’s behavior by an interaction of chemicals that he called “morphogens”. The sim-

This research was sponsored in part by Hewlett-Packard Laboratories, Palo Alto, California.

plest model uses two morphogens: the “activator” and the “inhibitor”. The morphogens themselves are produced by chemical reactions among particular enzymes in every cell of the animal’s skin during the animal’s embryonic stages [2].

According to this model, the two morphogens react with each other; however, the model consisting of reaction alone cannot account for the tremendous variety of coating patterns observed in animals. Since there is no inter-cellular flow of morphogens in the model, every cell acts as an independent autonomous system, producing the final morphogen concentrations based only on random initial concentrations. Therefore, cells end up in stable states that have no correlation or spatial structure, unlike the majority of patterns occurring in nature. In order to supplement the model with the needed transport mechanism, Turing incorporated a diffusion term into the system of equations. Thus, a typical reaction-diffusion system is a set of heat equations, coupled by non-linear reaction terms.

As a case study, Turing modeled the tentacle formation in hydra (a small tubular fresh-water polyp) with a 1-D reaction-diffusion system:

$$\begin{aligned}\frac{\partial \psi_A(x,t)}{\partial t} &= \psi_A(x,t) \cdot \psi_I(x,t) - \psi_A(x,t) - 12 \\ &+ q(x) + D_A \frac{\partial^2 \psi_A(x,t)}{\partial x^2}, \\ \frac{\partial \psi_I(x,t)}{\partial t} &= 16 - \psi_A(x,t) \cdot \psi_I(x,t) \\ &+ D_I \frac{\partial^2 \psi_I(x,t)}{\partial x^2},\end{aligned}\quad (1)$$

where $\psi_A(x,t)$ and $\psi_I(x,t)$ are the concentrations, and D_A and D_I are the diffusion rates of the activator and the inhibitor morphogens, respectively. The term $q(x)$, called the “evocator”, is a waveform of small random perturbations.

To gain a qualitative understanding of the operation of a two-morphogen reaction-diffusion system, consider two morphogens, the activator and the inhibitor, each reacting with itself and the other. While the reactions influence the local concentrations of the two morphogens, the diffusion transports the morphogens from cell to cell. Suppose the activator is auto-catalytic but diffuses slowly. In other words, its concentration increases in proportion to the amount already present, but its diffusion rate is low compared to that of the inhibitor. Thus the activator and the inhibitor create two opposing tendencies. On one hand, the activator concentration grows at a high rate locally, but does not spread fast enough to replace the inhibitor everywhere. On the other hand, the inhibitor consumes the activator at a low rate locally, but, because of its high diffusion constant, the inhibitor is delivered faster to remote sites, keeping the activator concentration finite everywhere. The competition between these two tendencies causes the concentration profiles of the activator and the inhibitor to settle into patterns of peaks and valleys.

We now summarize Turing’s analysis. The cells of hydra are assumed to be equally spaced and comprise a periodic 1-D lattice with the period of N_x cells. Using a popular discretization of the second derivative, followed by linearization around a fixed point, turns (1) into the equivalent

“small-signal” model:

$$\begin{aligned}\frac{\partial \psi_{A,s}(n_x,t)}{\partial t} &= 3\psi_{A,s}(n_x,t) + 4\psi_{I,s}(n_x,t) \\ &+ D_A[\psi_{A,s}(n_x+1,t) - 2\psi_{A,s}(n_x,t) \\ &+ \psi_{A,s}(n_x-1,t)], \\ \frac{\partial \psi_{I,s}(n_x,t)}{\partial t} &= -4\psi_{A,s}(n_x,t) - 4\psi_{I,s}(n_x,t) \\ &+ D_I[\psi_{I,s}(n_x+1,t) - 2\psi_{I,s}(n_x,t) \\ &+ \psi_{I,s}(n_x-1,t)],\end{aligned}\quad (2)$$

where the subscript “s” denotes a small deviation from the equilibrium value:

$$\psi_{A,eq}(n_x, t=t_0) = \psi_{I,eq}(n_x, t=t_0) = 4.$$

The combination of discretization and linearization has turned spatial derivatives into spatial convolutions, making the variables corresponding to different spatial indices in (2) intermixed. Variables are separated in a standard way by applying the Discrete Fourier Transform (DFT), turning convolutions into multiplications:

$$\begin{aligned}\frac{\partial \psi_{A,s}(k_x,t)}{\partial t} &= 3\psi_{A,s}(k_x,t) + 4\psi_{I,s}(k_x,t) \\ &- 4D_A\psi_{A,s}(k_x,t) \sin^2\left(\frac{\pi k_x}{N_x}\right), \\ \frac{\partial \psi_{I,s}(k_x,t)}{\partial t} &= -4\psi_{A,s}(k_x,t) - 4\psi_{I,s}(k_x,t) \\ &- 4D_I\psi_{I,s}(k_x,t) \sin^2\left(\frac{\pi k_x}{N_x}\right).\end{aligned}\quad (3)$$

The equations in (3) are a special case of the two-morphogen linear reaction-diffusion system of the form:

$$\begin{aligned}\frac{\partial \psi_{A,s}(k_x,t)}{\partial t} &= \psi_{A,s}(k_x,t) \left[r_{11} - 4D_A \sin^2\left(\frac{\pi k_x}{N_x}\right) \right] \\ &+ r_{12}\psi_{I,s}(k_x,t), \\ \frac{\partial \psi_{I,s}(k_x,t)}{\partial t} &= \psi_{I,s}(k_x,t) \left[r_{22} - 4D_I \sin^2\left(\frac{\pi k_x}{N_x}\right) \right] \\ &+ r_{21}\psi_{A,s}(k_x,t),\end{aligned}\quad (4)$$

where the diffusion rates, D_A and D_I , are restricted to be non-negative. The constants $r_{m_1 m_2}$ are called the marginal reaction rates. Depending on the eigenvalues and the initial conditions, the system (4) can exhibit six types of solutions, which are summarized in Table 1 for a 2×2 reaction-diffusion system.

The solution is a non-stationary spatial wave, unless $\lambda(k_x)$ is real. Both traveling wave and standing wave solutions are called non-stationary, because the amplitudes of such waves undergo sign changes.

Traveling waves cannot model an animal coat texture, because they do not produce a constant spatial pattern. Also, if the real part of $\lambda(k_x)$ is negative, then the spatial harmonics decay to zero. Thus, for explaining the formation of natural patterns, such as zebra stripes and leopard spots, it was the sixth mode (growing spatially-stationary waves) that received a lot of attention [2]. The other modes of reaction-diffusion systems have also been used, for instance, in modeling the behavior of oscillating chemical reactions [2].

The only mode of the system in (4) that is capable of producing stationary spatial waves is the one corresponding to $\lambda(k_x) \in \mathbb{R}$, $\lambda(k_x) > 0$ for some range of k_x . Since the amplitude of every k_x that belongs to this band of spatial frequencies grows as a function of time, the system becomes unstable for those values of k_x . Therefore, in order to produce stationary spatial waves, the system must be unstable for at least one spatial frequency. The harmonic $k_x = 0$ is excluded from the band of unstable wave numbers by definition. This maintains stable equilibrium levels in the absence of diffusion and guarantees that the system will be unaffected by homogeneous perturbations.

Turing has determined the conditions on D_A and D_I under which the system in (4) is stable to homogeneous (*i.e.*, DC) perturbations and unstable to non-homogeneous (*i.e.*, AC) perturbations at least for one value of k_x [1]. Turing gave the name “chemical wavelength” to this dominant spatial frequency, characteristic of (1).

As the amplitude of the dominant mode grows, the linear analysis ceases to be valid. However, Turing argues that the linear behavior predicts the overall non-linear behavior reasonably well. Subsequent computer simulations have confirmed this for many reaction-diffusion systems [8].

The present research emphasizes the use of reaction-diffusion models for synthesis and analysis of textures, regardless of whether or not every detail of the model considered is biologically plausible. Additionally, it has been shown that when discretized diffusion is replaced by a general finite impulse response (FIR) filter, even single-morphogen systems become capable of pattern formation [8]. This capability is utilized in applying the model to fingerprint restoration, which is described in Section 4.

3. M-LATTICE

A variety of non-linear reaction functions do not only facilitate local instabilities, essential for synthesizing textures, but also cause undesirable large-signal growth of state variables without bound. In order to alleviate this problem, while retaining the pattern-formation capabilities, we propose to study the reaction-diffusion system on a spatial grid and allow a general FIR filter in place of the discretized diffusion operator. By controlling the growth of the non-linear terms with a sigmoidal warping function, we arrive at the *M*-lattice system. As we show in Section 4, using a warping function does not destroy the small-signal behavior of the model, which is responsible for the formation of spatial patterns. Moreover, one can design the system such that the morphogen concentrations are bounded in the large-signal regime. The origin of the name “*M*-lattice system” comes from its roots in the reaction-diffusion paradigm, where *M* is the number of morphogens, or layers, in the lattice.

3.1. General Definition

Let $\psi_i(t) \in \mathbb{R}$ be a state variable as a function of time at each lattice point i , where $i = 1, \dots, N$. Let $\chi_i(t)$ be an output variable, obtained from $\psi_i(t)$ via $\chi_i(t) = g(\psi_i(t))$. The “warping” function, $g(u)$, an example of which appears in Figure 1, must be of a saturating type so as to limit the range of the output variables. Construct $\vec{\psi}(t)$ and $\vec{\chi}(t)$ by concatenating $\psi_1(t), \dots, \psi_N(t)$ and $\chi_1(t), \dots, \chi_N(t)$, respectively into column vectors.

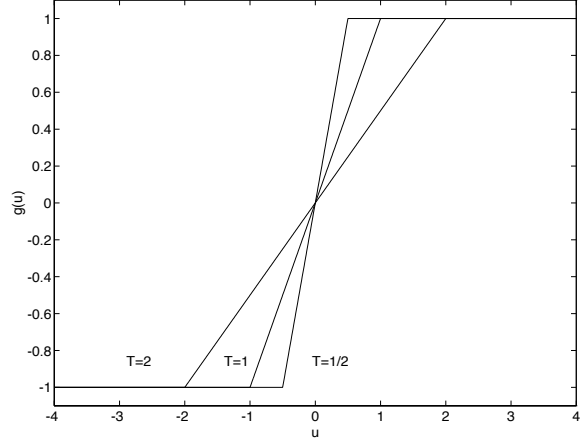


Figure 1: Plots of the clipping warping function for three different temperatures.

Definition 3.1 Suppose that the given functions, $f_i(\vec{\chi}(t))$, are continuous, differentiable, and bounded. Let the matrix \mathbf{A} be real with all eigenvalues having negative real parts: $\mathbf{A} \in \mathbb{R}^{N \times N}$, $\mathbf{A} = [a_{ij}]$, and $\forall i \Re(\lambda_i[\mathbf{A}]) < 0$. Define $\vec{f}(\vec{\chi}(t))$ by concatenating $f_1(\vec{\chi}(t)), \dots, f_N(\vec{\chi}(t))$ into a column vector. Then the *M*-lattice system¹ is a possibly non-linear autonomous dynamical system, described by the following equation:

$$\frac{d\vec{\psi}(t)}{dt} = \mathbf{A}\vec{\psi}(t) + \vec{f}(\vec{\chi}(t)). \quad (5)$$

A crucial property of the *M*-lattice system is that its state variables are bounded [8].

3.2. Clipped *M*-Lattice System

Consider the *M*-lattice, (5), with $\vec{f}(\vec{\chi}(t)) \stackrel{\text{def}}{=} \vec{\nabla}_{\vec{\chi}}\Phi(\vec{\chi}(t))$.

Definition 3.2 Suppose that the given function, $\Phi(\vec{\chi}(t))$, is continuous, twice-differentiable, and bounded. Let the matrix \mathbf{A} be real, symmetric, and negative-definite: $\mathbf{A} \in \mathbb{R}^{N \times N}$, $\mathbf{A} = [a_{ij}]$, $\mathbf{A} = \mathbf{A}^T$, and $\forall i \lambda_i[\mathbf{A}] < 0$. Then the clipped *M*-lattice system is the following possibly non-linear dynamical system:

$$\frac{d\vec{\psi}(t)}{dt} = \mathbf{A}\vec{\psi}(t) + \vec{\nabla}_{\vec{\chi}}\Phi(\vec{\chi}(t)). \quad (6)$$

As part of the analysis, we have shown that a subclass of the clipped *M*-lattice system possesses total stability, which is manifested in asymptotic convergence, regardless of the initial conditions [8]:

Proposition 3.1 Consider a special case of the *M*-lattice system, (6), in which $\mathbf{A} = \text{Diag} \{a_1, \dots, a_N\}$, $\forall i a_i < 0$. Any solution trajectory of this diagonal-state clipped *M*-lattice system converges to a finite asymptotically stable fixed point, $\vec{\psi} \in \mathbb{R}^N$ (or $\vec{\chi} \in [-1, 1]^N$).

¹This is the definition adapted for the present paper. The general *M*-lattice system is defined in [8].

Thus far, no proof of total stability exists for the more general system, (6). However, fixed points of the form $\vec{\chi} \in \{-1, 1\}^N$ are asymptotically stable [8]. In all experiments of the type that we discuss below, the general clipped M -lattice system exhibited convergence in computer simulation.

3.3. Comparison to Other Models

Several key aspects of the general M -lattice system, (5), with various saturating warping functions are unique when compared to other closely related models. Unlike the analog Hopfield network or the cellular neural network, the M -lattice system allows the \mathbf{A} matrix to have off-diagonal elements. In addition, the interactions among the output variables, $\chi_i(t)$ can in principle be described by a very general non-linear function, $\tilde{f}(\vec{\chi}(t))$. This flexibility enables the M -lattice system to capture the behavior of a wider variety of physical systems.

If \mathbf{A} is a diagonal matrix with negative elements on the main diagonal and $\Phi(\vec{\chi}(t))$ is a multilinear polynomial (*i.e.*, a polynomial whose independent variables have the powers zero or one [11]), then the M -lattice system with a sigmoidal warping function becomes the analog Hopfield network. For binary outputs, the M -lattice system, like the analog Hopfield network, is capable of optimization in the sense of the Hamming distance of one [11], [8].

If \mathbf{A} is a diagonal matrix with the same negative element on the main diagonal and $\vec{\nabla}_{\vec{\chi}}\Phi(\vec{\chi}(t))$ is a circulant (or block-circulant) symmetric matrix, which represents the convolution with a linear shift-invariant FIR filter, then the clipped M -lattice system, (6), becomes the original cellular neural network [10].

4. PRE-PROCESSING OF FINGERPRINTS

A typical fingerprint identification system contains a pre-processing step, which involves the restoration, enhancement, and halftoning of the original scanned and finely quantized fingerprint image. The essential steps comprising the identification sequence are: determining the type of the fingerprint, counting of ridges and bifurcations, and locating the core. A binary fingerprint image is more amenable for these tasks than a gray-scale fingerprint image [12].

We propose a pre-processing scheme that not only halftones the original fingerprint image, but also removes artifacts that can hinder the identification process. The method uses the ability of the clipped M -lattice system to excite locally-growing stationary spatial waves, which are the signature of reaction-diffusion systems, as well as to produce equilibrium images that have binary-valued pixels.

The motivation for using the reaction-diffusion aspect of the clipped M -lattice system is that fingerprint images have distinct patterns of thin curves, remotely resembling zebra stripes. Reinforcing the harmonics that create these curves will emphasize the essentials of the fingerprint, while suppressing the artifacts.

Let \mathbf{A} and \mathbf{H} be block-circulant symmetric matrices. Then the clipped M -lattice system, (6), can be written as follows:

$$\frac{d\psi(\vec{n}, t)}{dt} = a(\vec{n}) * \psi(\vec{n}, t) + s(\vec{n}) - h(\vec{n}) * \chi(\vec{n}, t), \quad (7)$$

where $\vec{n} \in \mathbb{Z}^2$, $a(\vec{n})$ and $h(\vec{n})$ are the FIR filters, corresponding to \mathbf{A} and \mathbf{H} , respectively, and $s(\vec{n}) \in [-1, 1]$ is the original finely quantized input image signal.

The advantage of using this type of the clipped M -lattice system for the pre-processing of fingerprints is that it can be guaranteed to produce binary outputs [8]. It now remains to demonstrate that (7) possesses the desired pattern-formation properties.

4.1. Small-Signal Regime: Reaction-Diffusion

Choose \mathbf{A} and \mathbf{H} such that the unique interior fixed point, $\psi(\vec{n}) \in (-1, 1)$, of (7) is at $s(\vec{n})$. Denote the DFT of the filters by $A(\vec{k})$ and $H(\vec{k})$. By Definition 3.2, it is necessary for the matrix \mathbf{A} , representing the linear term of the M -lattice system, to be made negative-definite. For the system in (7), \mathbf{A} is block-circulant and symmetric, containing $a(\vec{n})$ in the first row. Since the DFT basis consists of the eigenvectors of a block-circulant matrix, the $A(\vec{k})$ coefficients are proportional to the eigenvalues of \mathbf{A} , and therefore must be negative. Before $\psi(\vec{n}, t)$ reaches the clipping levels, (7) simplifies to:

$$\frac{d\psi(\vec{n}, t)}{dt} = s(\vec{n}) + \left(a(\vec{n}) - \frac{1}{T}h(\vec{n})\right) * \psi(\vec{n}, t). \quad (8)$$

Taking the DFT of both sides of (8) yields:

$$\frac{d\psi(\vec{k}, t)}{dt} = S(\vec{k}) + \left(A(\vec{k}) - \frac{1}{T}H(\vec{k})\right) \psi(\vec{k}, t), \quad (9)$$

whose solution for each \vec{k} is:

$$\psi(\vec{k}, t) = \left[S(\vec{k}) + \frac{S(\vec{k})}{F(\vec{k})}\right] \exp\{F(\vec{k})t\} - \frac{S(\vec{k})}{F(\vec{k})}, \quad (10)$$

where $F(\vec{k}) \stackrel{\text{def}}{=} A(\vec{k}) - \frac{1}{T}H(\vec{k})$, and the initial condition is set to $S(\vec{k})$, the DFT equivalent of the original image. Hence, from the discussion in Section 2, making $F(\vec{k})$ positive for a set of spatial frequencies creates the onset of growing spatially-stationary waves.

The adaptive filter, $H(\vec{k})$, was designed so as to include information about the dominant orientation at each pixel of the original image, shown in Figure 2(a) [13]. The dominant orientation at a pixel is characterized by the angle, $\theta_i \in [-\pi, \pi]$, and by the relative strength (or magnitude), $m_i \in [0, 1]$, of that angle's presence at pixel i . Each filter is a 2-D Gaussian, whose level sets are oriented ellipses. Denote the diagonal matrix of variances by \mathbf{V}_i , the rotation matrix by $\mathbf{\Theta}_i$, and the position vector by $\vec{n} \in \mathbb{Z}^2$:

$$\mathbf{V}_i = \begin{bmatrix} \sigma_{i,x}^2 & 0 \\ 0 & \sigma_{i,y}^2 \end{bmatrix}, \mathbf{\Theta}_i = \begin{bmatrix} \cos \theta_i & -\sin \theta_i \\ \sin \theta_i & \cos \theta_i \end{bmatrix}. \quad (11)$$

The relative sizes of $\sigma_{i,x}^2$ and $\sigma_{i,y}^2$ depend on m_i and determine the skewness of filters with respect to the dominant orientation:

$$\sigma_{i,y}^2 = \frac{L}{2}(1 - m_i), \quad \sigma_{i,x}^2 = L - \sigma_{i,y}^2, \quad (12)$$

where $L \times L$ is the size of the filter mask in pixels. Then the (unnormalized) oriented low-pass filter is given by:

$$h_i(\vec{n}) = \exp\{-\vec{n}^T \mathbf{\Theta}_i^T \mathbf{V}_i \mathbf{\Theta}_i \vec{n}\}. \quad (13)$$

Pertinent to fingerprint restoration is the kind of filtering that delineates the ridges, while canceling fluctuations in the DC level and getting rid of extraneous information. Thus, $H(\vec{k})$ and $A(\vec{k})$ are constructed so as to make the frequency bands corresponding to the ridges have negative DFT coefficients [14], and the $\frac{1}{T}$ factor amplifies the effect.

4.2. Large-Signal Regime: Halftoning

Figure 2(a) is a typical scanned and finely quantized fingerprint image from the NIST database [15]. The original image is 512×512 pixels and was low-pass filtered and down-sampled by a factor of 2 in each dimension in order to speed up the computation. From the figure, it can be seen that the original fingerprint is corrupted by a number of scratches, and several regions are obscured by uneven illumination. As shown in Figure 2(b), the common fingerprint halftoning method, based on adaptive median filtering and thresholding [12], only makes these artifacts more apparent, because it increases the image's contrast. The adaptive threshold is set to the average of the minimum and the maximum gray levels within some neighborhood surrounding each pixel of the original fingerprint image. The optimal size of the window was determined to be 5×5 pixels by trial and error.

There are two arguments in favor of using the clipped M -lattice system-based approach. First, the analysis of Section 4.1 implies that the attainable signal-to-noise ratios can be very large. Essentially, the clipped M -lattice system applies the filters, $a(\vec{n})$ and $h(\vec{n})$, an infinite number of times by the virtue of being a continuous-time system. Second, no separate halftoning step is needed, since the clipped M -lattice system binarizes the image.

Figure 2(c) displays the processed fingerprint image. The scratches have been removed and the unevennesses in the DC levels throughout the image have been eliminated. Essential detail such as ridges and bifurcations appear as continuous black curves, distinctly enhanced against a noise-free white background. Moreover, ridges and bifurcations have been extended even into the regions where they are barely detectable in the original image. This illustrates the celebrated synergetic property of reaction-diffusion systems: the emergence from noise of a spatial pattern, whose qualitative characteristics are pre-determined by the system's parameters. Using the Connection Machine (CM-2), the final image is produced in 25 iterations at the time step of 0.1 sec for the total time of less than 3 seconds or 1 minute including the system time and the I/O.

5. SUMMARY

We have reviewed the reaction-diffusion model, emphasizing its use of instability to form patterns. In an attempt to broaden the class of non-linear reaction functions that lead to bounded reaction-diffusion systems, we have introduced the M -lattice. We have shown that the clipped M -lattice is capable of synthesizing textured images by the same mechanisms as does the reaction-diffusion system.

The problem of simultaneous fingerprint restoration and halftoning is a natural application of the clipped M -lattice system, because of its ability to synthesize zebra stripes, which appear qualitatively similar to ridges and bifurcations found in human fingerprints. Incorporating orienta-

tion detection causes the clipped M -lattice system to act as an infinitely-aggressive band-pass filter. As a result, ridges are extracted at the highest contrast, even if they are only faintly detectable in the original image, while scratches, unevennesses in illumination, and other defects are removed.

6. REFERENCES

- [1] A. M. Turing, "The chemical basis of morphogenesis," *Phil. Trans. Royal Soc. London*, vol. 237, no. B, pp. 37-72, 1952.
- [2] J. D. Murray, *Mathematical Biology*. Berlin: Springer-Verlag, 1993.
- [3] A. Witkin and M. Kass, "Reaction-diffusion textures," *Computer Graphics*, vol. 25, pp. 299-308, July 1991.
- [4] G. Turk, "Generating textures on arbitrary surfaces using reaction-diffusion," *Computer Graphics*, vol. 25, pp. 289-298, July 1991.
- [5] C. B. Price, P. Wambacq, and A. Oosterlinck, "Applications of reaction-diffusion equations to image processing," in *Third Int. Conf. Image Proc. and App.*, (Warwick, UK), July 1989.
- [6] C. B. Price, P. Wambacq, and A. Oosterlinck, "Image enhancement and analysis with reaction-diffusion paradigm," *IEE Proc.*, vol. 137, June 1990.
- [7] A. Sherstinsky and R. W. Picard, " M -Lattice: A novel non-linear dynamical system and its application to halftoning," in *Proc. IEEE Int. Conf. Acoustics, Sp. Sig. Proc.*, vol. 2, (Adelaide, AU), pp. 565-568, Apr. 1994.
- [8] A. S. Sherstinsky, *M-Lattice: A System For Signal Synthesis And Processing Based On Reaction-Diffusion*. ScD thesis, Massachusetts Institute of Technology, Cambridge, MA, 1994.
- [9] J. J. Hopfield, "Neurons with graded response have collective computational properties like those of two-state neurons," *Proc. Nat. Acad. Sci., USA*, vol. 81, pp. 3088-3092, May 1984.
- [10] L. O. Chua and L. Yang, "Cellular neural networks: Theory," *IEEE Trans. on Circ. and Sys.*, vol. 35, pp. 1257-1272, Oct. 1988.
- [11] M. Vidyasagar, "Minimum-seeking properties of analog neural networks with multilinear objective functions," Tech. Rep. (Unpublished), Bangalore, India, 1993.
- [12] A. P. Russo, "An automatic system for fingerprint analysis," Master's thesis, Rensselaer Polytechnic Institute, Troy, NY, 1986.
- [13] W. T. Freeman and E. H. Adelson, "The design and use of steerable filters," *IEEE Trans. Pat. Anal. and Mach. Intell.*, vol. PAMI-13, pp. 891-906, Sept. 1991.
- [14] A. Sherstinsky and R. W. Picard, "Orientation-sensitive image processing with M -Lattice - a novel non-linear dynamical system," in *Proc. 1st IEEE Int. Conf. Image Proc.*, (Austin, TX), Nov. 1994.
- [15] National Institute of Standards and Technology, "Special database 4: 8-bit gray scale images of fingerprint image groups," July 1993.

class of wave	both $\Re[\lambda] < 0$ (stable)	either $\Re[\lambda] \geq 0$ (unstable)	λ	type of solution
traveling	decaying	growing	complex	oscillatory
standing	decaying (sum of a decaying traveling wave and its reflection)	growing (sum of a growing traveling wave and its reflection)	complex	oscillatory
stationary	decaying	growing	real	non-oscillatory

Table 1: Six modes admitted by a 2×2 reaction-diffusion system. The terms “decaying” and “growing” refer to the temporal behavior.

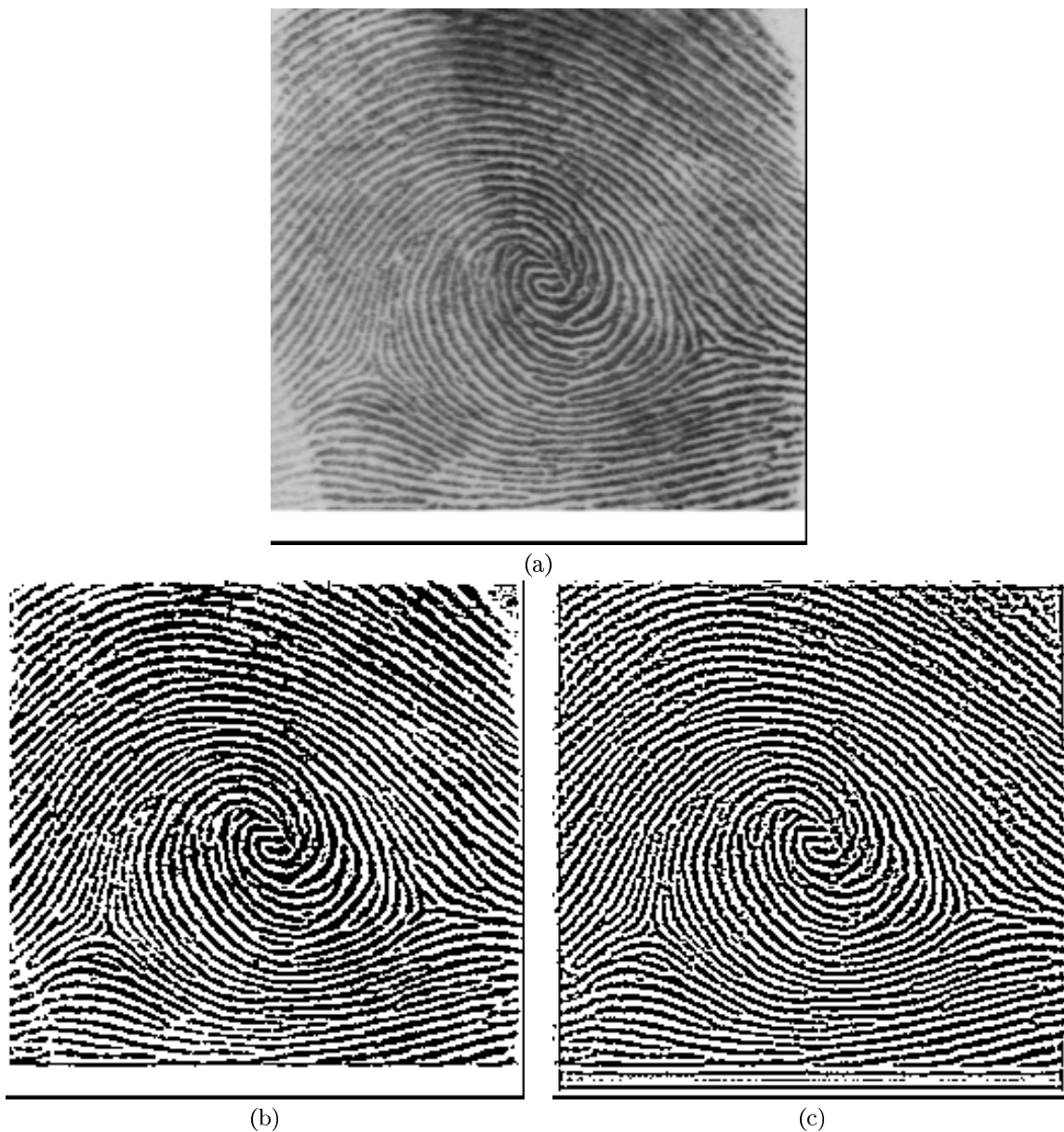


Figure 2: Restoration and halftoning of fingerprints. (a) the original “fingerprint” image; (b) the “fingerprint” image halftoned by a standard adaptive-threshold method; (c) the “fingerprint” image restored and halftoned by the clipped M -lattice system operating in the reaction-diffusion mode utilizing orientation information at each pixel of the original.